High Mass X-ray Binaries: illuminating the passage from massive binaries to merging compact objects
Proceedings IAU Symposium No. IAUS 346, 2019
L. Oskinova, E. Bozzo & T. Bulik, eds.

DOI: 00.0000/X000000000000000X

X-ray spectroscopy of massive stellar winds: previous and ongoing observations of the hot star ζ Pup

Miller, N.[1], Waldron, W.[2], Nichols, J.[3], Huenemoerder, D.[4], Dahmer, M.[5], Ignace, R.[6], Lauer, J.[7], Moffat, A.[8], Nazé, Y.[9], Oskinova, L.[10], Richardson, N.[11], Ramiaramanantsoa, T.[12], and Shenar, T.[13]

[1]U. of Wisconsin-Eau Claire, [2]Eureka Scientific, [3]Harvard-Smithsonian Center for Astrophysics, [4]MIT, [5]Northrop Grumman, [6]East Tennessee State U., [7]Harvard-Smithsonian Center for Astrophysics, [8]U. Montreal, [9]FNRS/U.Liège, [10]U. Potsdam, [11]U. Toledo, [12]Arizona State U., [13]KU Leuven

Abstract.
The stellar winds of hot stars have an important impact on both stellar and galactic evolution, yet their structure and internal processes are not fully understood in detail. One of the best nearby laboratories for studying such massive stellar winds is the O4I(n)fp star ζ Pup. After briefly discussing existing X-ray observations from Chandra and XMM, we present a simulation of X-ray emission line profile measurements for the upcoming 840 kilosecond Chandra HETGS observation. This simulation indicates that the increased S/N of this new observation will allow several major steps forward in the understanding of massive stellar winds. By measuring X-ray emission line strengths and profiles, we should be able to differentiate between various stellar wind models and map the entire wind structure in temperature and density. This legacy X-ray spectrum of ζ Pup will be a useful benchmark for future X-ray missions.

Keywords. stars: early-type, stars: mass loss, stars: winds, outflows, X-rays: stars

1. Introduction: Deep HETG spectrum of ζ Pup and multi-wavelength campaign 2018-2019

Massive stars have an important impact on the evolution and energy budget of a galaxy, producing comparable energy to a supernova over their ≈4 Myr lifetimes. The structure (including mass loss rates) and mechanisms of massive stellar winds have an important impact on galactic evolution, yet remain only partially understood. Our target here (ζ Pup (O4I(n)fp)) is one of the closest X-ray bright massive stars. XMM has long used ζ Pup as a reference target, so 18 years of observations are available from this spacecraft. These observations have been extensively analyzed in Nazé *et al.* (2012), Nazé *et al.* (2013), Hervé *et al.* (2013), and Nazé *et al.* (2018). One early Chandra HETG spectrum with a 67 kilosecond exposure is also currently available (Cassinelli *et al.* 2001).

The existing HETG spectrum hints at the interesting complexity of X-ray emission line profiles for this star. Even cursory inspection reveals that the observed line profiles greatly differ from the instrumental line spread function. However, insufficient photon counts per bin limited the utility of that spectrum to fully exploit the high spectral resolution of the HETG. We have therefore initiated a program to obtain unprecedentedly high S/N X-ray data for this star. With the HETG's high resolution and improved coverage of short wavelength lines (especially lines shortward of ≈8 Å), the spectra being obtained in this project will complement and extend current high S/N measurements performed with the RGS on XMM. The core of our program is 840 ks of Chandra HETG

spectral data to be taken over an 8-9 month period from July 2018 through early 2019. Some of the later X-ray spectra will be complemented by a contemporaneous multiwavelength campaign. Ground-based optical observations will occur in locations including Australia, New Zealand, SAAO, and CTIO. Space-based observations will take place using the BRITE constellation of satellites, providing us with a dual-band precision optical photometry time series during the relevant time period.

2. Line-Shape Models and Wind Properties

Winds of hot stars are believed to be propelled by an inherently unstable, line-driven process (Lucy & White 1980, Feldmeier 1995). It is thought that this instability allows small-scale perturbations in the wind to steepen into shocks. Interestingly, a recent investigation by Ramiaramanantsoa *et al.* (2018) found that these wind perturbations can be triggered by perturbations in the photosphere. After the wind perturbations form shocks, the resultant shock heating raises wind material to X-ray emitting temperatures. Due to Doppler broadening and wind absorption, we would expect asymmetric X-ray emission lines (Owocki *et al.* 1988, MacFarlane *et al.* 1991). Any detailed emission line model will need to include these effects, as discussed in Owocki & Cohen (2001), Cohen (2009), and Ignace (2016).

However, on the observational side, blue-shifted, asymmetric emission lines initially predicted by this scenario are in fact not commonly seen in hot stars, a situation referred to as the "line asymmetry problem" (Waldron & Cassinelli 2007). A number of investigations in recent years have made progress towards understanding the nature of this discrepancy for hot stars by exploring the ramifications of lower estimated mass loss rates (Oskinova *et al.* 2007, Cohen *et al.* 2014, Leutenegger *et al.* 2013, Oskinova 2016). Nonetheless, in some ways this paucity of profiles showing the initially expected widths and shifts gives those O stars which have asymmetric line profiles (such as ζ Pup) even more particular interest. The XMM observations of ζ Pup's X-ray emission lines have been analyzed by Hervé *et al.* (2013).

One important outstanding issue for understanding hot star X-ray emission line profiles is quantifying the presence and importance of inhomogeneities in the wind. Line profile models for different clumping properties can be seen in Oskinova *et al.* (2006). In that study, stellar wind properties were kept constant except for giving the winds different clumping properties. The large effects of clumping they find there illustrate the sensitivity of the X-ray line profiles as a probe for the structure of the wind. Another model including clumps is described in Leutenegger *et al.* (2013). For comparison, a typical smooth-wind model is described in Cohen *et al.* (2014).

The high resolution and long exposure time for the spectra in this investigation will allow us to perform detailed modeling of the X-ray emission line shapes. Analysis of mass loss rates, porosity (caused by clumps in the wind), and wind opacity will require very high S/N in each bin across each emission line. To explore the ability of observations to diagnose the importance of clumps, we simulated data for a no-clump case, and then fit it using a model which includes clumping. Because the simulated dataset is constructed with one model and the fit with an entirely different model, an examination of the residuals will indicate if an observation allows discrimination between the two cases. Figure 1 shows typical error bars and residuals for the existing 67 ks Chandra observation, while Figure 2 shows a simulation of the improvement expected when the full 840 ks Chandra observation is in hand. These figures illustrate how the increase in the S/N ratio of the observation will allow greater discrimination between models.

3. X-ray Temperature Distribution and Analysis of Weak Lines

The analysis of the overall spectral properties of hot stars is complicated by the line shape effects described in the previous sections. For many ordinary coronal X-ray sources X-ray emission lines are not broadened by bulk motions of the X-ray emitting plasma, but for hot stars the emission line shape must be understood to disentangle the contribution of each spectral line to each spectral bin. This is especially true in regions with many blends. After detailed line modeling is complete, the next step will be to determine line fluxes. An examination of the ratios of H-like to He-like lines of prominent elements can be used to obtain temperature information (Miller *et al.* 2002). This can be used with the f to i ratios of He-like ions probe the temperature structure in the wind, as described in Waldron & Cassinelli (2007).

In addition to previously-measured strong lines, there are many weak emission lines in ζ Pup's spectrum. These have been difficult to study in previous spectra due line blending in observations with insufficient exposure time to allow detailed modeling. For example, there are 50 lines in the 10-12 Å region that have T_x greater than 15 MK (mostly Fe lines). Also, He-like and H-like β lines for Ne, Mg, and Si, and weaker He-like Ar lines, and Ca lines may possibly be present. Additional Fe L shell lines may be measurable in this spectrum and would provide density diagnostic ratios. Measuring all the line strengths in this deep Chandra exposure will also allow accurate modeling and better determination of the overall temperature distribution of the X-ray emitting plasma.

4. X-ray Variability

XMM shows variability for ζ Pup on a timescale of days in the total band, which may reflect the presence of CIRs (Nazé *et al.* 2018, Nazé *et al.* 2013). Temporal variation in the X-ray emission from hot stars might also be expected due to the growth and fading of shocks. The XMM data for this star was examined for this kind of variation (Nazé *et al.* 2013). We will be exploring this Chandra dataset for line strength and profile variations over time. This Chandra dataset will especially allow us to analyze the temporal behavior of shorter-wavelength emission lines and will allow us to probe all emission lines at higher resolution. In 2019 we will be observing ζ Pup nearly contemporaneously with both earth- and space-based optical telescopes to probe for correlated temporal variation between the X-ray and optical bands. These parallel observations will allow us to see if the X-rays are modulated on the same 1.78 d timescale found in the optical by Howarth & Stevens (2014). In a recent analysis Ramiaramanantsoa *et al.* (2018) were able to map bright surface features and their associated CIRs which had periodicity on this time scale, firmly connecting this 1.78 day period with stellar rotation. The exploration of related variability on this timescale could provide an important link between features on the photosphere and structures in the wind.

References

Cassinelli, J.P., Miller, N.A., Waldron, W.L., MacFarlane, J.J., Cohen, D.H., 2001 ApJ 554, 55L
Cohen, D.H., 2009, AIP Conference Proceedings 1161
Cohen, D., Wollman, E., Leutenegger, M., Sundquist, J., Fullerton, A., Zsargo, J., Owocki, S., 2014, ApJ 586, 495
Feldmeier, A., 1995 A&A 299, 523
Hervé, A., Rauw, G., & Nazé, Y. 2013, A&A, 551, A83
Howarth, I.D., Stevens, I.R., 2014 MNRAS 445, 2878
Ignace, R., 2016, Adv. Sp. Res. 58,694

Leutenegger, M., Cohen, D., Sundquist, J., Owocki, S.., 2013, ApJ 770,80
Lucy, L.B., White, R.L., 1980 ApJ 241, 300
MacFarlane, J.J., Cassinelli, J.P., Walsh, B.Y., Vedder, P.W., Vallerga, J.V., Waldron, W.L., 1991 ApJ 380, 564
Miller, N.A., Cassinelli, J.P., Waldron, W.L., MacFarlane, J.J., Cohen, D.H. 2002 ApJ 577, 951
Nazé, Flores, C.A., Rauw, G., A&A 538, A22
Nazé, Y., Oskinova, L., Gosset, E., 2013 ApJ 763,143
Nazé, Y., Ramiaramanantsoa, T., Stevens, I. R., Howarth, I. D., & Moffat, A. F. J. 2018, A&A, 609, A81
Oskinova, L.M., Hamann, W.-R., Feldmeier, A., 2006, MNRAS 372,313
Oskinova, L. M., Hamann, W.-R., Feldmeier, A. 2007 A&A 476, 1331
Oskinova, L.M., 2016 Adv. Sp. Res. 58, 679
Owocki, S.P., Castor, J.L., Rybicki, G.B., 1988 ApJ 335, 914
Owocki, S.P., & Cohen D. H, 2001 ApJ 559, 1108
Puls, J., Markova, N., Scuderi, S., Stanghellini, C., Taranova, O. G., Burnley, A. W., Howarth, I. D. 2006, A&A, 454, 625
Ramiaramanantsoa, T., Moffat, A. F. J., Harmon, R., et al. 2018, MNRAS, 473, 5532
Waldron, W.L., & Cassinelli, J.P., 2007 ApJ 668, 456

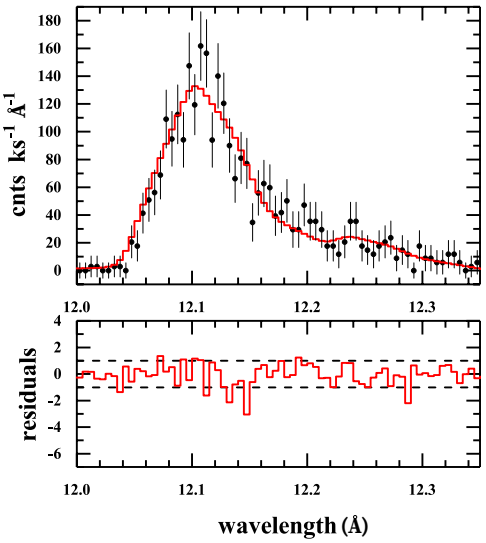

Figure 1. Comparison of the MEG Ne X region clump model (solid line) to a simulated smooth wind dataset with errors appropriate to the existing 2000 HETG observation. The large errors per bin make it difficult to make precise determinations of the model parameters, and there is no clear pattern in the residuals. The residuals are in the sense of (model) minus (simulated model) divided by the simulated error for each bin. This diagram is constructed using the standard bin size for the MEG detector (0.005 Å).

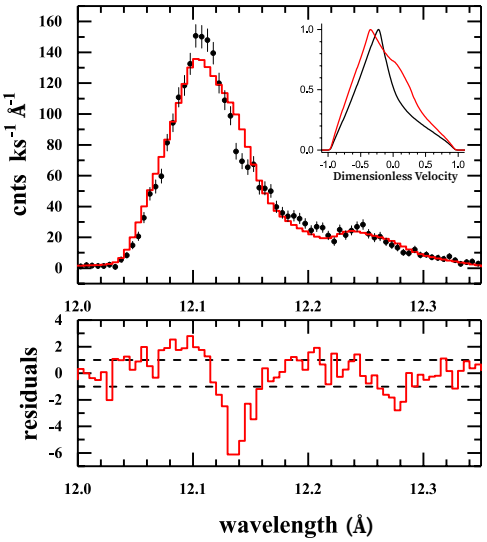

Figure 2. Same as Figure 1 except this panel illustrates a simulation of the precision we expect for the spectrum using the full approved Cycle 19 Chandra exposure time. This will greatly enhance our ability to differentiate models as evident in the clear trends which are apparent in the simulated residuals. The inset shows the theoretical line shapes for the smooth wind (black) and clumped (red) models before the inclusion of any instrumental effects. The normalized theoretical line profile models in the inset are displayed as a function of the dimensionless velocity (i.e. the line-of-sight wind velocity divided by the terminal velocity, with 0 representing the rest wavelength for the line). This calculation assumes a value of 2250 km s^{-1} for the terminal velociy (Puls *et al.* 2006).